



Image Restoration Techniques in Super-Resolution Reconstruction of MRI images

Hisham A. Alsayem¹, Yasser M. Kadah²

¹Faculty of Engineering, Cairo University, Cairo, Egypt, E-mail: Hesham.elsayem@eng.cu.edu.eg

²Electrical and Computer Engineering Department, King Abdulaziz University, Jeddah, Saudi Arabia

ABSTRACT

Increasing the resolution of the MRI scans results in lowering the signal-to-noise ratio and/or increasing the scan time. In this paper, we improved the resolution of MRI images by obtaining a high resolution image from a sequence of low resolution images using the super-resolution reconstruction methodology. Image restoration is an important step in the reconstruction process, the final appearance and the quality of the reconstructed image depend greatly on the restoration method used. In this paper, we evaluated the performance of three restoration techniques used in the reconstruction, the first one is based on truncated singular value decomposition, the second one is based on Tikhonov regularization and the last one is based on total variation. Experiments are performed on synthetic images and real MRI brain images to verify the results obtained from the numerical simulations.

Keywords: Magnetic resonance imaging, super-resolution, image restoration, regularization

I. INTRODUCTION

Medical imaging plays an important role in the diagnosis of the diseases and therefore it is crucial to obtain a high quality medical image. Here the quality is determined by the spatial resolution, the high resolution (HR) images contain more details which facilitates the process of the diagnosis. Upgraded imaging systems can produce HR images but this requires a high cost also the resolution affects other imaging parameters. In MRI increasing the resolution reduces the signal-to-noise ratio (SNR) and/or increases the acquisition time [1]. In order to tackle this issue, super-resolution reconstruction (SRR) is used to reconstruct the HR image [2]. SRR is the process of creating a HR image from a sequence of observed low resolution (LR) images, the idea behind SRR is to combine the different information of LR images to reconstruct one HR image. The LR images contain different information because there are sub-pixel shifts between them. Comprehensive recent studies that provide explanation to the SRR problem and its algorithms can be found in [3], [4]. SRR methodology has been applied recently to MRI [5], [6], [7] to improve the pictorial information of the scans. Nonuniform interpolation approach is one of SRR algorithms which reconstructs the final HR image by applying three image processing steps successively. These steps are registration of the LR frames, interpolation on a HR grid and image restoration process to remove the blurring and the noise introduced by the system [2]. A previous study on SRR in MRI in [8] provided qualitative results for the success of this approach but did not assess the performance of the restoration techniques when applied to MRI data.

In this paper, we address SRR problem in medical imaging using the nonuniform interpolation algorithm with three different restoration techniques including truncated singular value decomposition (TSVD) [9], Tikhonov regularization [10]-[11], and total variation (TV) regularization [12]. The algorithm is applied on both synthetic images (Shepp-Logan phantom) and real MRI brain images and to evaluate the performance of the used restoration techniques we measured the peak signal-to-noise ratio (PSNR) and the Structural Similarity Index (SSIM) to the generated HR image.

II. THE SUPER-RESOLUTION PROBLEM AND THE RECONSTRUCTION METHOD

In SRR problem an imaging model should be constructed to know the relation between the original HR image and the degraded LR images. The assumed imaging model is shown in Fig. 1. Assuming that the true HR image is x and the k^{th} LR image is y_k , then the acquisition model which contains the degradations introduced by the MRI machine can be written in a linear form as:

$$y_k = DBMx + n_k, \quad (1)$$

where M is a warp matrix, B is a blur matrix, D is a sub sampling matrix and n is an additive white Gaussian noise with $\text{SNR} > 3$ as shown in [13]. So, the problem is how to reconstruct the MRI image x from the observed data y .

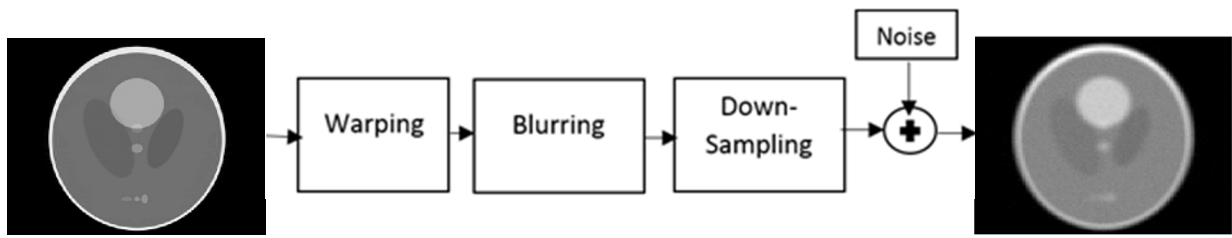


Fig. 1: The imaging model used in our study, HR image on the left and LR image is on the right.

Nonuniform interpolation is a SRR algorithm which states that if B is a linear shift invariant blur and M represents only a simple motion like translation and rotation then x can be reconstructed from the set y by first, registration of the LR frames. Second, interpolation is done on a HR grid. Finally, image restoration process to remove the blurring and the noise. The steps of the algorithm are shown in Fig. 2. The success of the whole process depends greatly on the registration accuracy so it is important to use a good method, in our study we used the method described in [14]. We applied bicubic interpolation for the registered frames on the HR grid. The image restoration is ill-posed inverse problem and therefore we used regularization techniques as described in the next section.

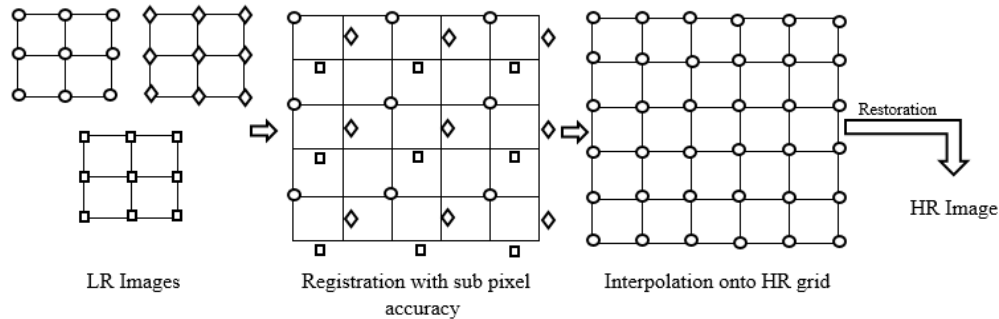


Fig. 2: The Nonuniform interpolation method.

III. IMAGE RESTORATION TECHNIQUES

The goal of image restoration is to restore the original scene from its degraded version. The degradation is often due to a linear blur and an additive random noise. The degraded image can be described mathematically as:

$$g = Hf + w, \quad (2)$$

where H is a known linear blur matrix, g and f are the degraded and the original image vectors respectively written in lexicographical notation, and w is a term represents the additive random noise. If the matrix H is a square matrix, then its singular value decomposition (SVD) can be defined as:

$$H = U\Sigma V^T, \quad (3)$$

where U and V are orthogonal matrices and ($\Sigma = \text{diag}(\sigma_i), i = 1, \dots, N$) is a diagonal matrix whose diagonal contains positive numbers σ_i that appear in descending order. These numbers are called the *singular values* of the matrix H . The naïve way to get an estimation to the original image f can be written as:

$$\hat{f}_{\text{naive}} = H^T g. \quad (4)$$

However, this estimation is unreliable and usually gives unsatisfactory result because it is sensitive to noise. The noise dominates the solution due to the small singular values of the matrix H [9]. So, regularization techniques should be used to stabilize the solution.



A. Truncated Singular Value Decomposition (TSVD)

The TSVD is a regularization technique that solves the problem by taking only the first $t < N$ singular values and discarding the other smaller ones. The TSVD of H can be defined as:

$$H_t = U_t \Sigma_t V_t^T . \quad (5)$$

U_t contains only t column vectors of U , V_t^T contains only t row vectors of V^T and Σ_t contains only the largest t singular values. The regularized solution can be estimated as:

$$\hat{f} = H_t^{-1} g . \quad (6)$$

This estimation gives a good result which is not dominated by the noise. In our study the optimal value of t is calculated by the generalized cross validation (GCV) method [15].

B. Tikhonov Regularization

In this technique, the regularized solution is defined as the minimizer of the following equation:

$$\underset{\hat{f}}{\text{minimize}} \frac{1}{2} \|H\hat{f} - g\|_2^2 + \lambda \|L\hat{f}\|_2^2, \quad (7)$$

where L is the regularization matrix, λ is the regularization parameter and $\|\cdot\|_2$ is the 2-norm. The first term measures the fidelity to the data and the second term is the side constraint which represents the prior knowledge about the solution. The minimization of (7) can be expressed as:

$$H^T g = (H^T H - \lambda L^T L) \hat{f} . \quad (8)$$

The parameter λ determines the amount of the regularization on the solution. In our study The optimal value of λ is calculated by GCV method.

C. Total Variation (TV) Regularization

This method is a popular regularization technique that preserves the edges of the restored image, we consider the following two mathematical problems [12]:

The TV/L2 minimization:

$$\underset{\hat{f}}{\text{minimize}} \frac{1}{2} \|H\hat{f} - g\|_2^2 + \|\hat{f}\|_{TV}, \quad (9)$$

and the TV/L1 minimization:

$$\underset{\hat{f}}{\text{minimize}} \lambda \|H\hat{f} - g\|_1 + \|\hat{f}\|_{TV}, \quad (10)$$

where λ is the regularization parameter, $\|\cdot\|_2$ is the 2-norm, $\|\cdot\|_1$ is the 1-norm, and $\|\hat{f}\|_{TV}$ is defined as:

$$\|\hat{f}\|_{TV} = \sum_k \sqrt{[H_u \hat{f}]_k^2 + [H_v \hat{f}]_k^2} . \quad (11)$$

$[A]_k$ refers to the k^{th} entry of the vector A , H_u and H_v are the gradient operators along the horizontal and the vertical directions respectively. To solve these problems we used the algorithm described in [12] which uses the augmented Lagrangian method.

IV. EXPERIMENTAL VERIFICATION

The discussed SRR approach has been applied to both synthetic images and human MRI brain images. Six synthetic images were simulated by applying the following successive operations on the Shepp-Logan phantom of size (256×256):

- 1) Global Translation.
- 2) Gaussian blurring.
- 3) Down sample by factor of two (Size = 128×128).
- 4) Add Gaussian random noise with SNR = 30 dB.

Now we have a group of shifted, blurred, down-sampled and noisy images and the problem is to restore the original HR image from this sequence. Also The LR brain images of MRI were with the same characteristics. The PSNR of the reconstructed image is defined as:

$$PSNR = 10 \log_{10} \left(\frac{255^2}{Mean - Squared - Error (MSE)} \right) dB, MSE = \frac{\sum [\hat{x}(i, j) - x(i, j)]^2}{(256)^2}. \quad (12)$$

Here, $\hat{x}(i, j)$ is the reconstructed image and $x(i, j)$ is the original image. Another image quality metric that will be used is the Structural Similarity Index (SSIM), which assesses the visual impact of luminance, contrast and structure of an image given as [17]:

$$SSIM(x, y) = \frac{(2\mu_x\mu_y + C_1)(2\sigma_{xy} + C_2)}{(\mu_x^2 + \mu_y^2 + C_1)(\sigma_x^2 + \sigma_y^2 + C_2)} \quad (13)$$

Where μ_x , μ_y , σ_x , σ_y , and σ_{xy} are the local means, standard deviations, and cross-covariance for images x and y , while C_1 and C_2 are the regularization constants for luminance and contrast terms (taken by default as $C_1 = (0.01 \times \text{Dynamic Range})^2$ and $C_2 = (0.03 \times \text{Dynamic Range})^2$) [17]. The PSNR and SSIM are computed for the reconstructed HR image to evaluate the success of different SRR methods. Such metrics also help evaluate the performance of the different super resolution restoration techniques when applied to MRI data.

V. RESULTS AND DISCUSSION

Six synthetic LR images were used to reconstruct the HR image of size (256×256). The mean squared error of the registration result was (0.0013, 0.0024) pixels which is a small error and does not affect the reconstruction process. The reconstructed HR images are shown in Fig. 3 and their PSNR/SSIM values are given in Table 1. Another experiment was performed using real MRI brain images, Six LR MRI images were used to reconstruct a HR image with size (256×256). The resultant images are shown in Fig. 4 and their PSNR/SSIM values are provided in Table 2.

From Fig. 3 and Fig. 4, the proposed method performed well to generate a HR image with clear structures from a set of degraded LR images by applying the non-uniform interpolation algorithm. Also, the values of the PSNR/SSIM presented in Table 1 and Table 2 provide quantitative evidence. All the restoration techniques gave acceptable results in terms of good pictorial information and PSNR/SSIM metrics. The solution of TSVD used only approximately 48,000 singular values from the total 65,536 singular values in the case of the Shepp-Logan phantom and used only approximately 10,000 singular values in the case of MRI brain images. As shown in Fig. 3(b) and Fig. 4(b), noise did not dominate the reconstructed images because the effect of the small singular values was eliminated. When the matrix L in Tikhonov regularization is the identity matrix, the side constraint represents the energy of the image f . This means that the energy of the image is minimized by excluding too large pixel values from the solution and λ controls the tradeoff between the fidelity to the data and the energy of the solution. The results in this case were quite similar to the results of TSVD, whereby this similarity was shown in many literatures such as [16]. When the matrix L is the Laplacian operator, which is a high-pass filter, the side constraint measures the roughness of the solution. This means that the prior knowledge about the solution is the smoothness and λ controls the tradeoff between the fidelity to the data and the smoothness of the solution. The assumption of the smoothness constraint is usually valid for most medical images. As demonstrated by the results, the results when L is the Laplacian operator were better than the results when L is the identity matrix because this operator imposed smoothness on the result and hence the noise was reduced. In TSVD and Tikhonov regularization, GCV technique determined the optimal regularization parameter which resulted in obtaining an optimal solution that best eliminates

the noise and fits the data. TV regularization is a very good method for image restoration where this method preserved the edges and suppressed the noise resulting in restored images with a clear appearance. The TV/L1 minimization was more suitable to the problem than the TV/L2 because it has higher PSNR/SSIM as seen in Table 1. TV regularization does not assume the smoothness of the information and hence the result was rather blocky and the edges were preserved. This was not the case in Tikhonov regularization, which assumes smoothness.

From the point of view of computational complexity, the run time for both of Tikhonov and TSVD methods in our experiments took less than 0.025 seconds, while the TV-based methods took an average time of 0.3 seconds. The experiments were performed on a modest computing platform with MATLAB R2010a running on a 64-bit Microsoft Windows 8 and an Intel® Core™ i3 processor at 2.27GHz and 2 GB RAM. Therefore, the computational complexity of the proposed methods is expected to meet real-time performance requirements on modern computational platforms. Even though there may appear that the TV-based methods have a disadvantage of their order of magnitude higher computation time, such difference will not involve noticeable delays with the present data rates of MRI systems. Hence, this indicates the potential of these methods for practical applications.

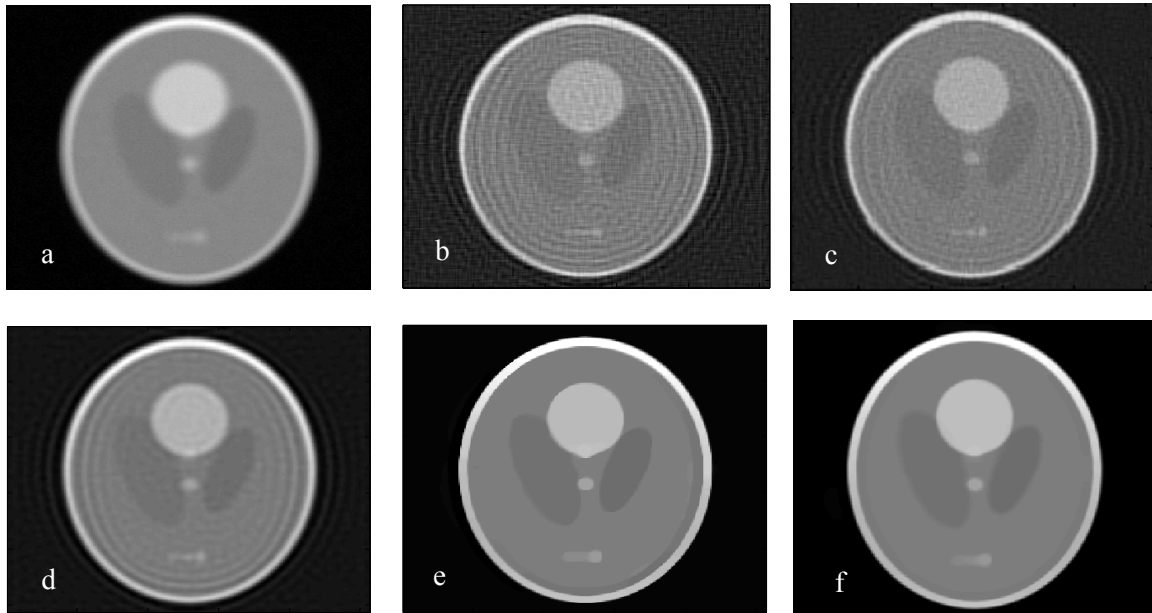


Fig. 3: The input data and the reconstructed images by different restoration techniques. (a) One of the LR images, (b), (c), (d), (e) and (f) are HR images with size (256×256) reconstructed by TSVD, Tikhonov with $L=I$, Tikhonov with $L = \text{Laplace operator}$, TV/L1 minimization and TV/L2 minimization, respectively.

Table 1: The PSNR and SSIM of the Reconstructed HR Images of Shepp-Logan phantom by Different Restoration Techniques

Restoration Method	PSNR (dB)	SSIM
TSVD	31.81	0.76
Tikhonov, $L=I$	31.24	0.75
Tikhonov, $L=\text{Laplace operator}$	34.90	0.88
TV/L1	35.20	0.92
TV/L2	32.99	0.87

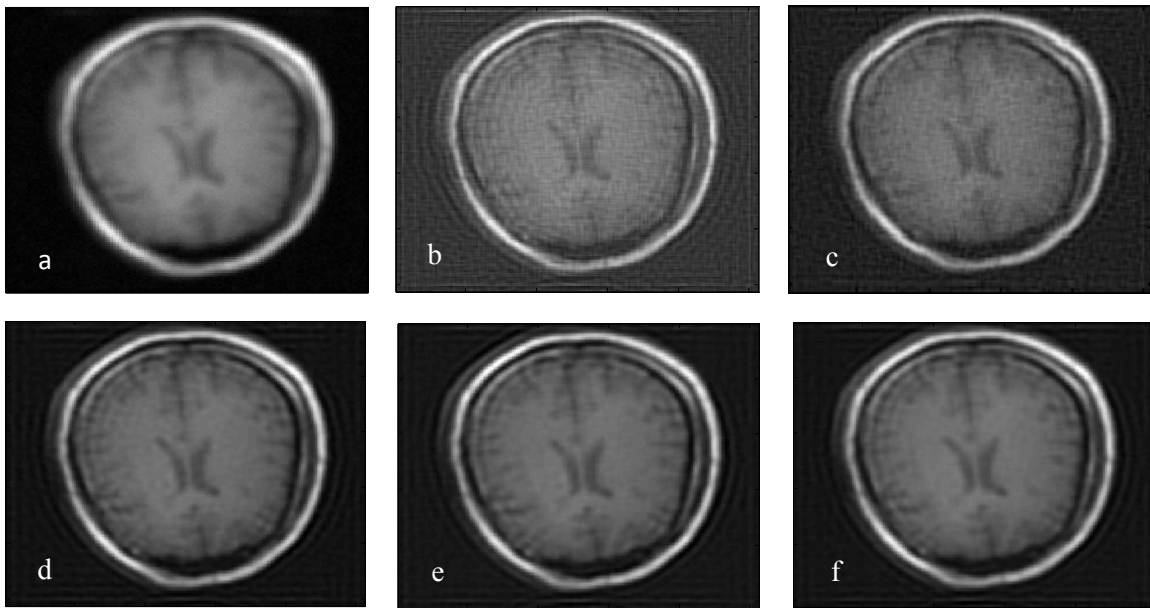


Fig. 4: The images of SRR of MRI images. (a) One of the LR images, (b), (c), (d), (e) and (f) are HR images with size (256×256) reconstructed by TSVD, Tikhonov with $L=I$, Tikhonov with L = Laplace operator, TV/L1 minimization and TV/L2 minimization, respectively.

Table 2: The PSNR and SSIM of the Reconstructed MRI Brain Images by Different Restoration Techniques

Restoration method	PSNR (dB)	SSIM
TSVD	30.00	0.73
Tikhonov, $L=I$	30.27	0.71
Tikhonov, L =Laplace operator	34.70	0.88
TV/L1	34.90	0.91
TV/L2	31.60	0.82

VI. CONCLUSIONS

In this work, the reconstruction of high resolution medical images using SRR was achieved without reducing the SNR or increasing the scan time. Three restoration techniques were proposed in the nonuniform interpolation SRR approach. We compared their performance as applied in the proposed SRR framework on both simulated and real medical images. The PSNR/SSIM metrics of the reconstructed images were used in the quantitative comparison between the restoration methods. The results indicated that the TV regularization is more efficient in image restoration. This emphasizes the importance of choosing appropriate restoration technique in determining the quality of the reconstruction.

REFERENCES

- [1] E. M. Haacke, R. W. Brown, M. R. Thompson, and R. Venkatesan, *Magnetic Resonance Imaging: Physical Principles and Sequence Design*. New York: John Wiley Sons, 1999.
- [2] S. C. Park, M. K. Park, and M. G. Kang, "Super-Resolution Image Reconstruction: a Technical Overview," *IEEE Sig Proc Mag*, vol. 20, no. 3, pp. 21–36, 2003.
- [3] K. Nasrollahi, and T. B. Moeslund, "Super-Resolution: A Comprehensive Survey." *Mach Vis Appl*, vol. 25, no. 6, pp. 1423–1468, 2014.
- [4] P. B. Chopade, and P. M. Patil, "Single and Multi Frame Image Super-Resolution and its Performance Analysis: A Comprehensive Survey." *Int J Comput Appl*, vol. 111, no. 15, Feb. 2015.
- [5] S. Peled and Y. Yeshurun, "Superresolution in MRI: Application to human white matter fiber tract visualization by diffusion tensor imaging," *Magn. Reson. Med.*, vol. 45, no. 1, pp. 29–35, 2001.
- [6] H. Greenspan, G. Oz, N. Kiryati, and S. Peled, "MRI inter-slice reconstruction using super-resolution," *Magn. Reson. Imaging*, vol. 20, no. 5, pp. 437–446, 2002.



- [7] A. Carmi, S. Liu, N. Alon, A. Fiat, and D. Fiat, "Resolution enhancement in MRI," *Magn. Reson. Imaging*, vol. 24, no. 2, pp. 133–154, 2006.
- [8] D. Van Reeth, I. W. K. Tham, C. H. Tan, and C. L. Poh, "Super-resolution in magnetic resonance imaging: A review," *Concept Magnetic Res - Part A*, vol. 40A, no. 6, pp. 306–325, 2012. [Online]. Available: <http://dx.doi.org/10.1002/cmr.a.21249>
- [9] P. Hansen, J. Nagy, and D. O'Leary, *Deblurring Images: Matrices, Spectra, and Filtering (Fundamentals of Algorithms 3)*. Philadelphia, PA: SIAM, 2006.
- [10] D. L. Phillips, "A technique for the numerical solution of certain integral equations of the first kind," *J. ACM*, vol. 9, pp.84-97, 1962.
- [11] N. Tichonov, "Solution of incorrectly formulated problems and the regularization method", *Soviet Math. Dokl.*, vol. 4, pp. 1035 -1038, 1963
- [12] S. H. Chan, R. Khoshabeh, K. B. Gibson, P. E. Gill, and T. Q. Nguyen, "An augmented Lagrangian Method for Total Variation Image Restoration," *IEEE Trans. Image Process.*, vol. 20, no. 11, pp.3097–3111, 2011.
- [13] H. Gudbjartsson and S. Patz, "The Rician distribution of noisy MRI data," *Magn. Reson. Med.*, vol. 34, no. 6, pp. 910–914, 1995.
- [14] P. Vandewalle, S. Süssstrunk, and M. Vetterli, "A frequency domain approach to registration of aliased images with application to super-resolution," *EURASIP J. Appl. Sig Proc*, vol. 2006, pp. 1–14, 2006.
- [15] P. C. Hansen, *Rank-Deficient and Discrete Ill-Posed Problems*, Philadelphia: SIAM, 1998.
- [16] A.C. Bovik, *Handbook of Image and Video Processing*, Academic Press: New York, 2000.
- [17] <http://www.mathworks.com/help/images/ref/ssim.html>. (accessed on December 13, 2015).